Science Advances

AAAS

advances.sciencemag.org/cgi/content/full/4/3/eaar3566/DC1

Supplementary Materials for

Terahertz electrical writing speed in an antiferromagnetic memory

Kamil Olejník, Tom Seifert, Zdeněk Kašpar, Vít Novák, Peter Wadley, Richard P. Campion, Manuel Baumgartner, Pietro Gambardella, Petr Němec, Joerg Wunderlich, Jairo Sinova, Petr Kužel, Melanie Müller, Tobias Kampfrath, Tomas Jungwirth

Published 23 March 2018, *Sci. Adv.* **4**, eaar3566 (2018)
DOI: 10.1126/sciadv.aar3566

This PDF file includes:

- section S1. Terahertz current calibration
- section S2. Temperature dependence of the relaxation
- section S3. Heat-assisted nature of the reversible switching
- fig. S1. Comparison of switching at 300 and 260 K.
- fig. S2. Device temperature with the pulse on.

section S1. Terahertz current calibration

To obtain the absolute current density scale in the THz writing speed experiments, as quoted for the data in Figs. 3B,4A and shown in the inset of Fig. 6B of the main text, we used calibration measurements in the contact setup summarized in Fig. 6C. The heat-assisted switching of our devices shows a transition in the characteristic Joule energy density ϵ required to obtain a reference switching signal of, e.g., 1 mΩ. It changes from a steeply decreasing ϵ with increasing $1/\tau_p$ below $\sim$ MHz to a saturated value of ϵ in the GHz range. (Note that this change in trend correlates with the observation of a $1/\tau_p$ - independent pulse-induced temperature rise of the CuMnAs bit cell below a MHz writing speed and a temperature rise that decreases with increasing $1/\tau_p$ for higher speeds (*16*).) The characteristic Joule energy density for the device breakdown follows an analogous trend and also saturates in the GHz range, as shown in Fig. 6C. This provides the basis for our experimental E to j conversion in the THz writing speed experiments. Specifically, we associate the measured value of the breakdown THz field E with the device breakdown energy in the saturated regime the value of which was determined in the GHz writing speed experiments. From the expression $\epsilon = j^2\tau_p/\sigma$ and for $\tau_p \approx 1$ ps we then obtain the value of the breakdown current density j corresponding to the breakdown THz field E. This provides us with the E to j conversion factor which scales with the bit cell size and which we apply to the switching data measured at the THz writing speed. We note that the relatively small separation between writing and breakdown energies in our device geometry provides additional confidence in our experimental procedure for inferring the switching current densities in the non-contact THz writing speed measurements.

section S2. Temperature dependence of the relaxation

In fig. S1 we show switching experiments with trains of 100 μs pulses and subsequent relaxation at 300 K and 260 K measured in the same CuMnAs structure as in Fig. 3 in the main

text. While at room temperature we observe partial relaxation of the signal, no relaxation is observed in this CuMnAs structure already when slightly lowering the temperature to 260 K. We note that, in general, the stability of the switching signal can be broadly varied by changing the CuMnAs structure parameters (*16*) and examples of stable retention at room temperature in analogous electrical switching experiments in Mn_2Au are shown, e.g., in Ref. *19*.

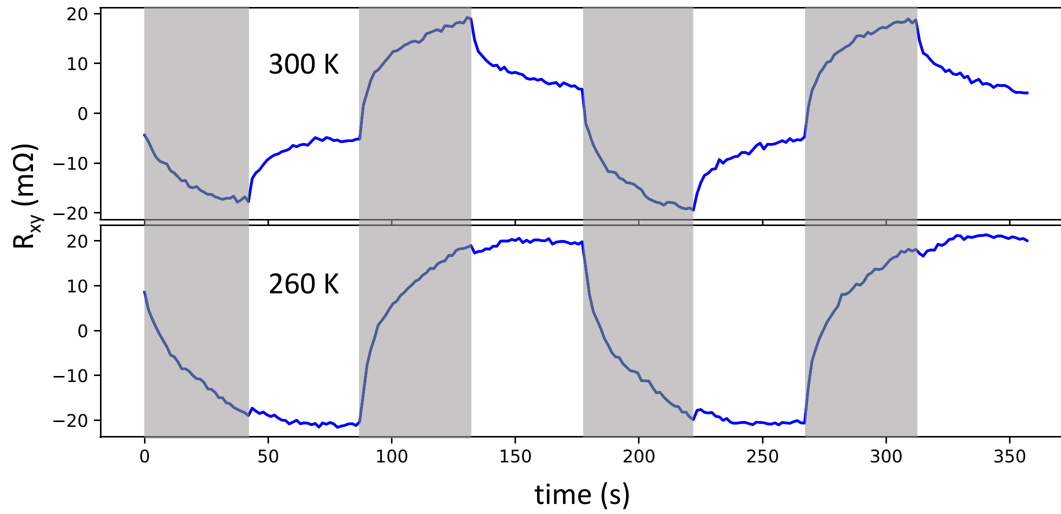

fig. S1. Comparison of switching at 300 and 260 K. Examples of switching by trains of 30 pulses within 45 s with individual pulse-length of 100 μs and alternating orthogonal writing current directions (grey regions), and of signal relaxation within 45 s with the pulse-train turned off (light regions) at (A) base temperature 300 K and writing current density 1.6×10^7 Acm^{-2} and (B) base temperature 260 K and writing current density 2.2×10^7 Acm^{-2}.

section S3. Heat-assisted nature of the reversible switching

In the left panel of fig. S2 we show an example of temperature evolution determined from resistance measured during a 100 μs long writing pulse. We observe fast increase of the temperature in the first ~ 10 μs followed by a saturated regime. This saturation of temperature is connected with establishing thermal gradient in the substrate below the device resulting in an effective heat outflow. The right panel of fig. S2 shows the current density needed to write a 5 mΩ signal

and the temperature T_{end} of the device at the end of the pulse, both as a function of the base temperature T_{base}. The current density increases significantly with decreasing base temperature while the temperature at the end of the pulse is similar. This highlights the heat-assisted nature of the reversible switching by the staggered current-induced field in our devices. It is also consistent with the observed saturation of the writing energy at shorter pulses during which heat does not have time to dissipate from the device. In this regime the transient increase of sample temperature during the pulse can be expected to scale with the delivered energy.

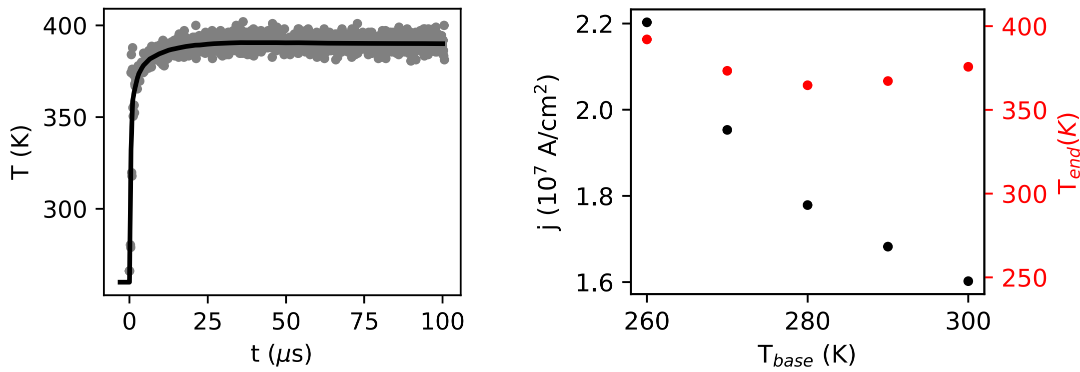

fig. S2. Device temperature with the pulse on. Left panel: Example of the evolution of the temperature of the device determined from resistance measurements during a 100 μs long writing pulse of current density 2.2×10^7 Acm^{-2} and base temperature 260 K. Right panel: Current density (black) needed to write a 5 mΩ signal and temperature of the device at the end of the writing pulse (red) as a function of the base temperature.